

Theoretical Study of Ni(N₄)₂, Ni(C₄H₄)₂, and Ni(C₂O₂)₂ Complexes

Qian Shu Li* and Jun Guan

School of Chemical Engineering and Materials Science, Beijing Institute of Technology, Beijing 100081, China

Received: December 8, 2002; In Final Form: July 30, 2003

Ab initio molecular orbital theory and density functional theory have been applied to study the isoelectronic-liganded NiL₂ (L = N₄²⁻, C₄H₄²⁻, and C₂O₂²⁻) sandwich complexes at the MP2/6-31G*, B3LYP/6-31G*, B3LYP/6-311+G*, and B3LYP/6-311+G(3df,3pd) levels of theory. The stable structure for Ni(N₄)₂ is a staggered conformer with *D*_{4d} symmetry. The dissociation barriers for one N₂ elimination and two N₂ eliminations for Ni(N₄)₂ are 37.1 and 84.9 kcal/mol, respectively, at the B3LYP/6-31G* level of theory, which suggest that Ni(N₄)₂ is kinetically stable enough to resist dissociation. The calculated reaction energies for the dissociation of Ni(N₄)₂, Ni(C₄H₄)₂, and Ni(C₂O₂)₂ at the B3LYP/6-31G* level of theory suggest that both Ni(N₄)₂ and Ni(C₂O₂)₂ are high-energy species; however, Ni(C₄H₄)₂ is not.

1. Introduction

In the past decades, pure nitrogen clusters have been noticed by the idea that pure nitrogen molecules may be used as possible candidates for environmentally friendly high-energy density materials (HEDMs).^{1–6} However, more and more hypothetical stable structures of pure nitrogen clusters have recently been questioned about their possibilities of being used as HEDMs because of their kinetic instabilities.^{7–11} Therefore, other stable forms of polynitrogens were explored. Wilson et al.¹² quantitatively showed how four- and six-membered nitrogen rings could be stabilized by coordinating covalent bonds to oxygen. Gagliardi and Pyykö predicted the structure and stability of ScN₇.¹³ Subsequently, they reported N₅MN₇ (M = Ti, Zr, Hf, and Th), N₅ScN₇, and N₅VN₇ with a total charge of 0, -1, and +1, respectively.¹⁴ The dissociation barriers, 20 kcal/mol for ScN₇ and 21.5 kcal/mol for N₅ThN₇, indicate that both of these two species have the chance of existing. Straka¹⁵ theoretically suggested the possibility of stabilizing the N₆ species as a planar hexagonal ring in MN₆ (M = Ti, Zr, Hf, and Th) systems. Fe(N₅)₂ was reported by Lein et al.¹⁶ to have a strong metal–ligand interaction. This iron bispentazole is an energy-rich compound, lying 226.8 kcal/mol higher in energy than its most stable dissociation products of an iron atom and five N₂ molecules. Analogous to the reported Fe(N₅)₂, in which the N₅⁻ is a planar aromatic ring, the N₄²⁻ planar ring might be stabilized as a π -system ligand by the interaction between a ligand and a transition metal atom. Previous research on N₄²⁻ has been reported.^{15,17} The N₄²⁻ was predicted to be a *D*_{4h}-symmetric planar-square anion. Moreover, in the neutral CaN₄¹⁵ and bipyramidal Li₂N₄,¹⁷ N₄²⁻ remains planar. On the basis of the previous studies,^{1–21} structure and thermodynamic and kinetic stability of a hypothetical Ni(η^4 -N₄)₂ sandwich complex were investigated in the present paper. Because Ni(C₄H₄)₂ and Ni(C₂O₂)₂ are isoelectronic with Ni(N₄)₂, it is also interesting to see their thermodynamic stabilities and compare the bonding nature between them. Therefore, the geometries, energies, harmonic vibrational frequencies, and the nature of bonding of the isoelectronic-liganded complexes Ni(C₄H₄)₂ and Ni(C₂O₂)₂ were also investigated in the present study.

2. Methods

Geometries and harmonic vibrational frequencies of all complexes were calculated using density functional theory (DFT) and second-order perturbation theory (MP2) methods at the B3LYP/6-31G*, B3LYP/6-311+G*, B3LYP/6-311+G(3df,3pd), and MP2/6-31G* levels of theory, where B3LYP is a DFT method using Becke's three-parameter nonlocal functional²² along with the Lee–Yang–Parr nonlocal correlation functional (LYP)²³ and B3LYP is a “half-and-half” HF/DFT hybrid exchange functional (BH)²⁴ with the LYP²³ model for correlation. The MP2 method uses the frozen core approximation.²⁵ The 6-31G* is a standard split-valence double- ζ polarization basis set,²⁶ and 6-311+G* is a split-valence triple- ζ plus polarization basis set augmented with diffuse functions.²⁷ Natural bond orbital^{28–31} (NBO) analysis was carried out at the B3LYP/6-31G* level of theory based on the optimized geometries at the same level of theory. Minimum-energy pathways connecting the reactants and products were confirmed using the intrinsic reaction coordinate (IRC) method with the Gonzalez–Schlegel second-order algorithm.³² Throughout this paper, bond lengths are provided in angstroms, bond angles in degrees, total energies in hartrees, and relative energies and zero-point vibrational energies, unless otherwise stated, in kcal/mol. All calculations were performed with the Gaussian 98 program package.³³

3. Results and Discussion

The molecular structures, along with their optimized geometrical parameters, for Ni(N₄)₂, Ni(C₄H₄)₂, and Ni(C₂O₂)₂ are illustrated in Figures 1, 2, and 3, respectively. Figure 4 shows the molecular structures for the transition states and dissociation products, along with their optimized geometrical parameters. The qualitative frontier molecular orbital correlation diagrams for the interactions between the ligand and Ni⁴⁺ for Ni(N₄)₂, Ni(C₄H₄)₂, and Ni(C₂O₂)₂ are shown in Figures 5–7, respectively. The total energies, zero-point vibrational energies (ZPE), and number of imaginary vibrational frequencies are listed in Table 1. The relative energies with ZPE corrections are given in Table 2. Table 3 shows the dissociation energies of the homolytic bond cleavage. Harmonic vibrational frequencies and IR intensities for Ni(N₄)₂ (*D*_{4d}), Ni(C₄H₄)₂ (*D*_{4d}), and Ni(C₂O₂)₂ (*D*_{2d}) are shown in Table 4.

* To whom correspondence should be addressed. Fax: +86-10-6891-2665. E-mail: qqli@bit.edu.cn.

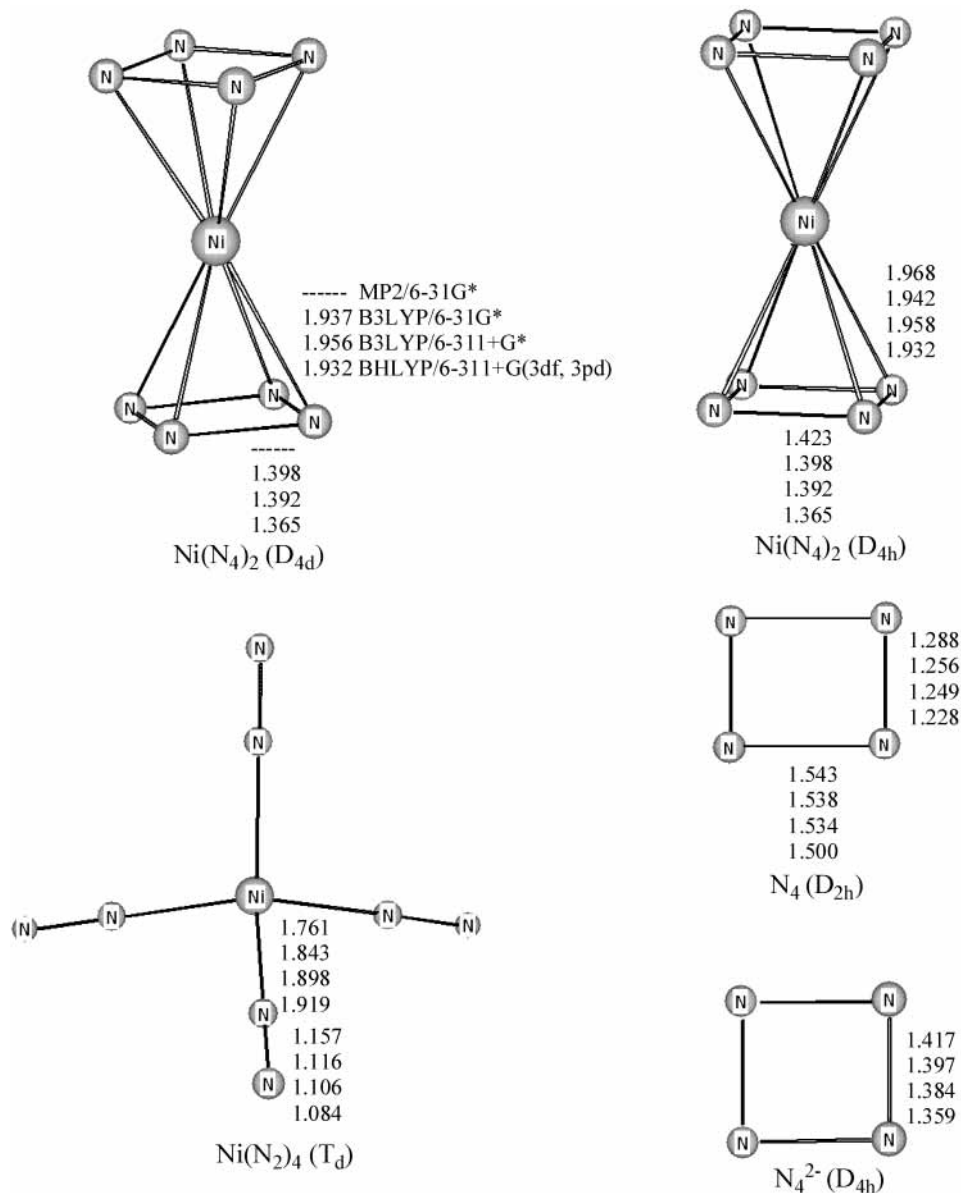


Figure 1. Optimized molecular structures, along with their geometrical parameters, for Ni(N₄)₂ (D_{4d}), Ni(N₄)₂ (D_{4h}), Ni(N₂)₄ (T_d), N₄ (D_{2h}), and N₄²⁻ (D_{4h}).

The calculations predict that the stable structure of Ni(N₄)₂ is a staggered conformer with D_{4d} symmetry, rather than an eclipsed one with D_{4h} symmetry. For the two conformers, the latter is a transition state with one small imaginary vibrational frequency, being only 0.6 kcal/mol less stable than the former at the B3LYP/6-31G* level of theory. When larger basis sets 6-311+G* (at the B3LYP level of theory) and 6-311+G(3df, 3pd) (at the BHLYP level of theory) were used, the energy difference between the staggered and eclipsed conformers of Ni(N₄)₂ becomes extremely slight (as listed in Table 2), which suggests that there is probably no internal barrier for the rotation of the two N₄²⁻ ligands about the C₄ axis. In our calculations, we have attempted to optimize the D_{4d}-symmetric structure at the MP2/6-31G* level of theory; however, we failed in finding it. From Table 2, we can see that the differences of the relative energies obtained at the above three different levels of theory are also slight. As shown in Figure 1, the bond length of N–N in Ni(N₄)₂ (the following discussions focus on the conformation of D_{4d} symmetry, unless otherwise stated) is 1.398 (B3LYP/6-31G*), 1.392 (B3LYP/6-311+G*), and 1.365 Å (BHLYP/6-311+G(3df,3pd)), which is close to the bond length of N₄²⁻

(D_{4h}) (1.397, 1.384, and 1.359 Å at the above three levels of theory, respectively). The bond-length equalization, which is the sign of aromaticity for hydrocarbons,³⁴ has also been observed in Ni(N₄)₂. Moreover, according to NBO analysis, the calculated Wiberg bond indices (WBI) for all N–N bonds in Ni(N₄)₂ are 1.2, indicating delocalization. The bond length of Ni–N in Ni(N₄)₂ is 1.937 (B3LYP/6-31G*), 1.956 (B3LYP/6-311+G*), and 1.932 Å (BHLYP/6-311+G(3df,3pd)). The covalent radius value for nitrogen is 0.70³⁵ or 0.75 Å,³⁶ while that for nickel is 1.21 Å.³⁶ It is clear that the calculated Ni–N bond length in Ni(N₄)₂ lies between the two sums of the covalent radii of nickel and nitrogen (1.91 and 1.96 Å). At the B3LYP/6-31G* level of theory, Mulliken charge analysis shows that all positive charges lie on the nickel (about +0.64) while all negative charges populate on the nitrogens (about –0.08 per N atom). Moreover, the WBIs for all Ni–N bonds are about 0.4. According to the calculation results listed above, it seems that the metal–ligand bonds are possibly partly ionic and partly covalent.

Thermodynamically speaking, Ni(N₄)₂ is a local minimum on its potential energy surface. To assess its stability further,

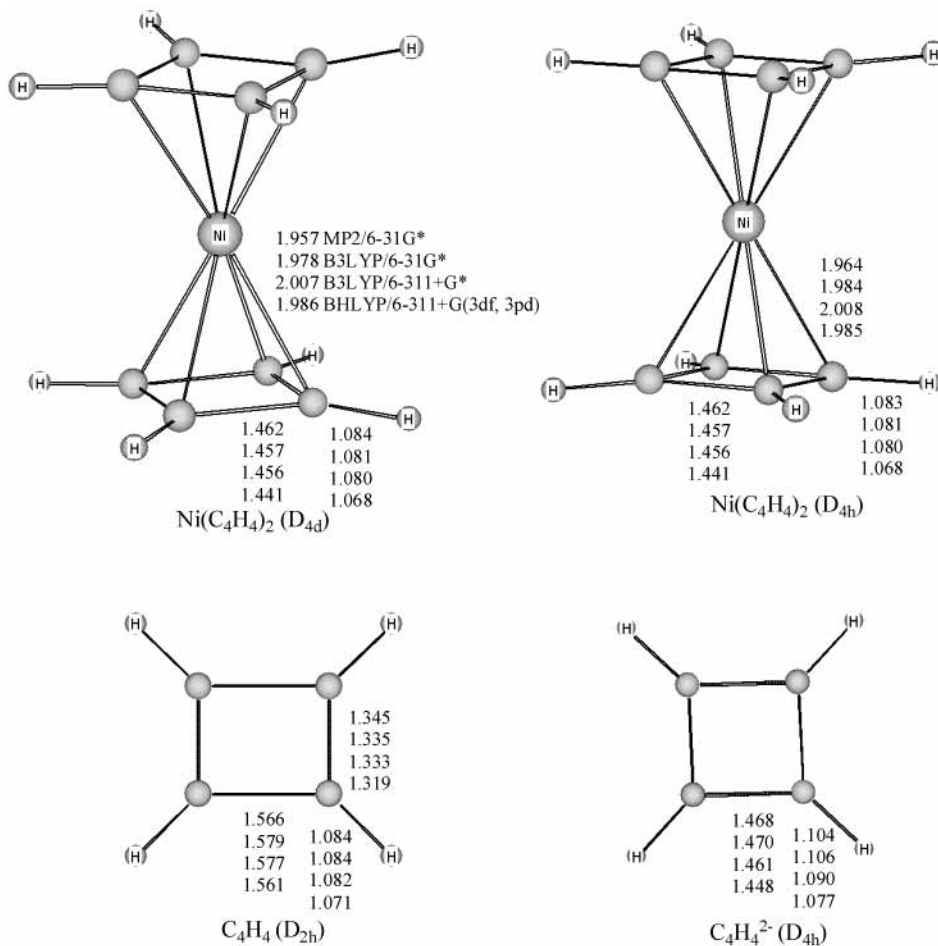


Figure 2. Optimized molecular structures, along with their geometrical parameters, for Ni(C₄H₄)₂ (D_{4d}), Ni(C₄H₄)₂ (D_{4h}), C₄H₄ (D_{2h}), and C₄H₄²⁻ (D_{4h}).

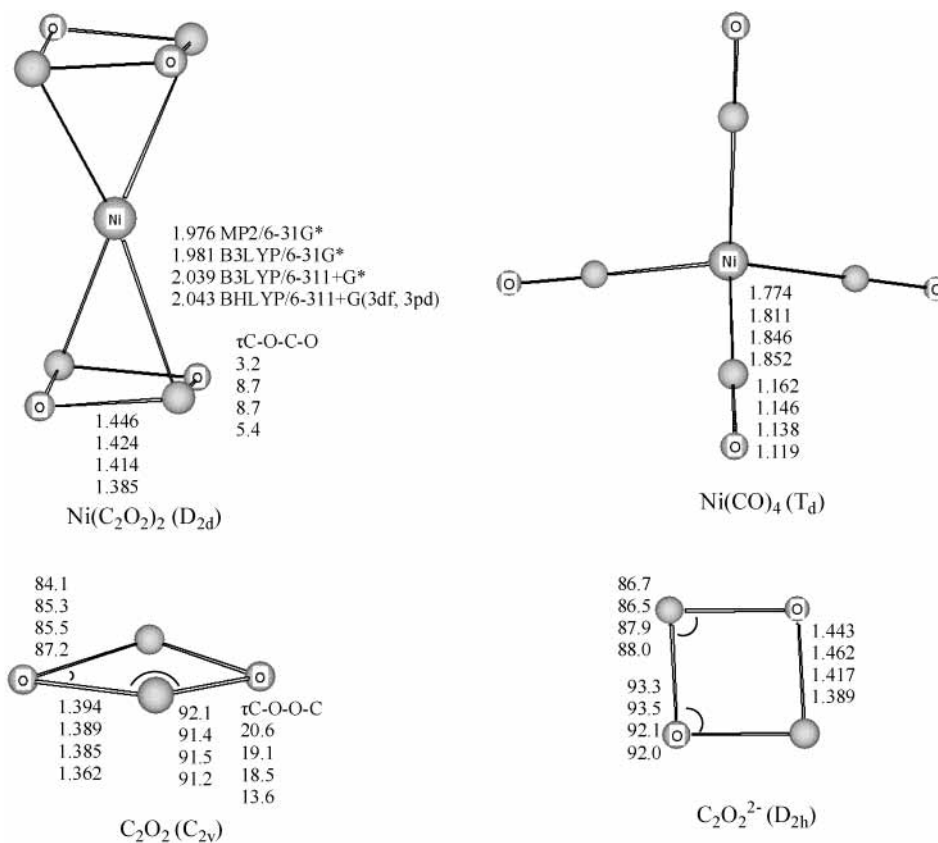


Figure 3. Optimized molecular structures, along with their geometrical parameters, for Ni(C₂O₂)₂ (D_{2d}), Ni(CO)₄ (T_d), C₂O₂ (C_{2v}), and C₂O₂²⁻ (D_{2h}).

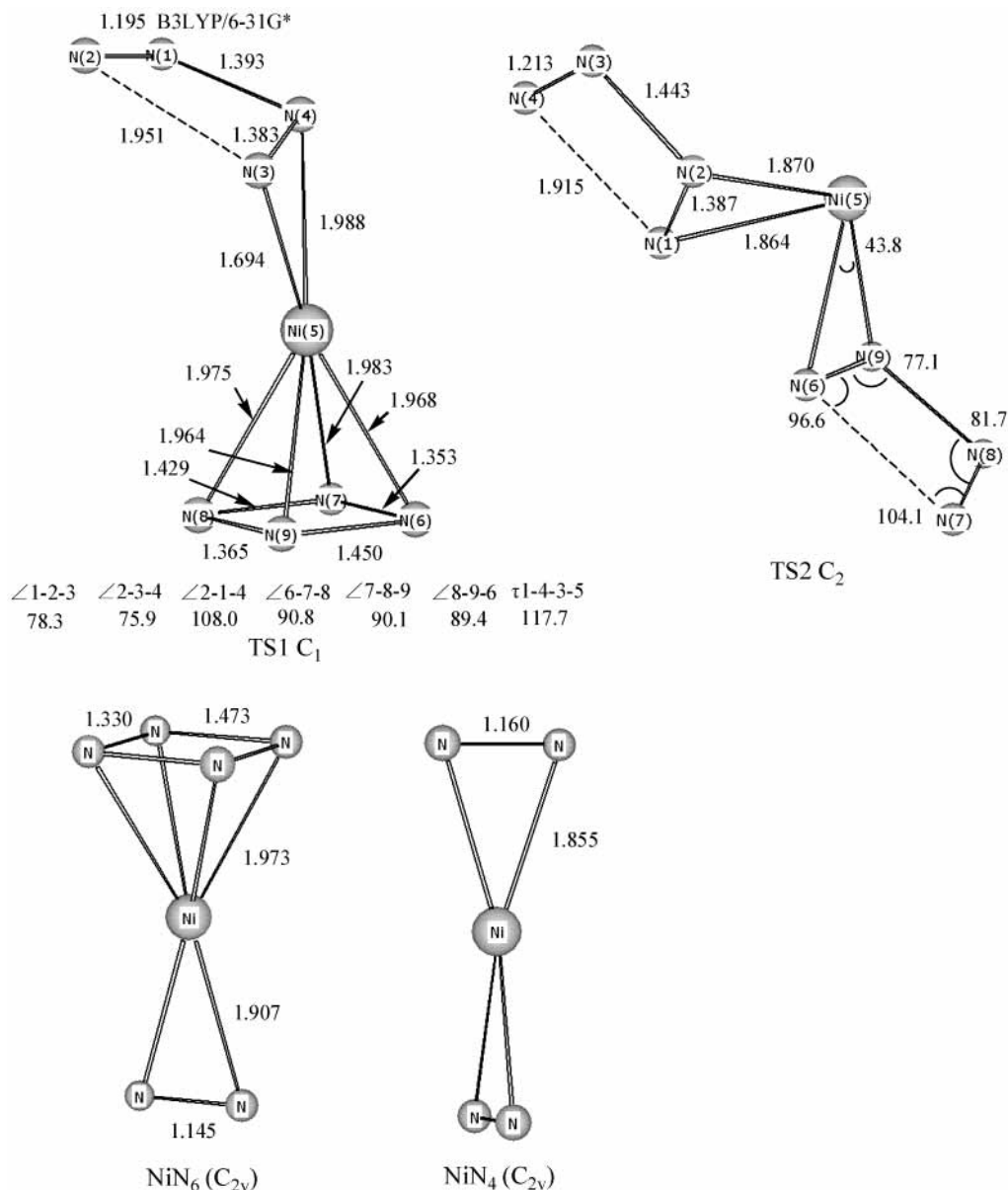


Figure 4. Optimized molecular structures, along with their geometrical parameters, for the transition states (TS1 and TS2) and dissociation products (NiN₆ (C_{2v}) and NiN₄ (C_{2v})).

the dissociation reactions were investigated at the B3LYP/6-31G* level of theory. As shown in Figure 4, two transition states (TS1, TS2) were found on the potential energy surface. TS1 corresponds to one N₂ elimination and TS2 corresponds to two N₂ eliminations, lying 37.1 and 84.9 kcal/mol above Ni(N₄)₂, respectively, at the B3LYP/6-31G* level of theory with ZPE corrections. Such high dissociation barriers may be attributed to its strong ligand ↔ metal interaction. The high dissociation barriers suggest that Ni(N₄)₂ should be stable enough to resist decomposition. The IRC calculation confirms that TS1 is connected to Ni(N₄)₂ on the reactant side and to NiN₆ (C_{2v}) and N₂ on the product side. Moreover, the IRC path suggests that there is a ring slippage, which brings the hapticity from η⁴ to η² before the N₂ molecule starts to pull out. On the other hand, starting from TS2, the IRC leads to NiN₄ (C_{2v}) and two N₂ molecules. From the results presented here, it can be inferred that the elimination of N₂ molecules is a stepwise process. In addition, concerning possible interactions with the environment, such as other ligands (e.g., H⁻, OH⁻, and OR⁻), we looked into the energy levels of the frontier orbitals of Ni(N₄)₂ at the

B3LYP/6-31G* level of theory. The energy levels of the frontier orbitals are -8.94 and -4.62 eV for the HOMO and LUMO of Ni(N₄)₂, respectively. For a comparison, the energy levels of the frontier orbitals of Ni(C₄H₄)₂ (HOMO, -5.23 eV; LUMO, -0.64 eV) and Ni(C₂O₂)₂ (HOMO, -7.71 eV; LUMO, -3.81 eV) were also examined at the same level of theory. The large HOMO-LUMO gaps for these three complexes suggest that they all may be thermodynamically stable. The lower LUMO for Ni(N₄)₂ suggests that it would be chemically more reactive as a Lewis acid than Ni(C₄H₄)₂ and Ni(C₂O₂)₂. Therefore Ni(N₄)₂ may be more prone to act as an electrophile than Ni(C₄H₄)₂ and Ni(C₂O₂)₂ in chemical reactions.

To compare the stabilities of Ni(N₄)₂ with the recently predicted ScN₇, ThN₆, N₅ThN₇, and Fe(N₅)₂, we investigated the energy release of Ni(N₄)₂ at the B3LYP/6-31G* level of theory, considering a Ni atom and four N₂ molecules as possible final dissociation products. The predicted ScN₇ lies about 36 kcal/mol per N₂ unit higher in energy above a Sc atom and 7/2 N₂.¹³ For ThN₆, it lies about 24 kcal/mol per N₂ unit above the energy of a Th atom and 3N₂.¹⁵ The energy of N₅ThN₇ lies

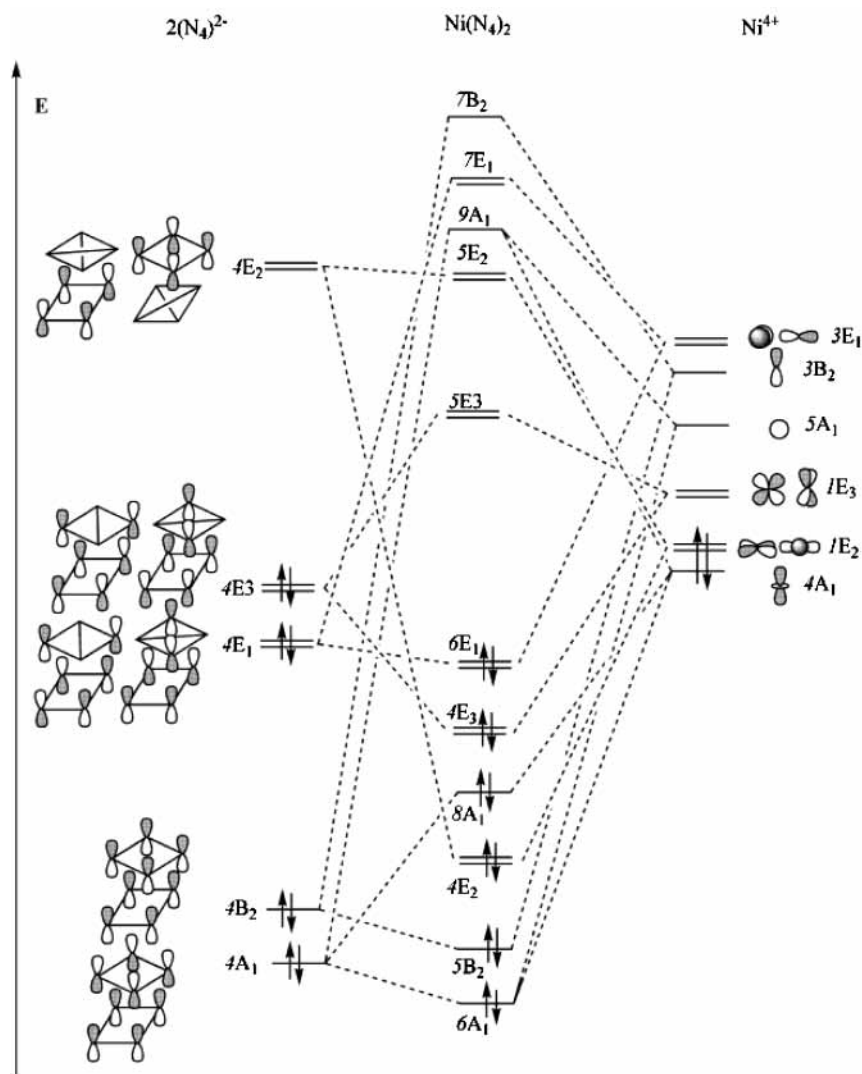


Figure 5. A qualitative frontier molecular orbital correlation diagram for $\text{Ni}(\text{N}_4)_2$ (D_{4d}).

22 kcal/mol per N_2 unit higher than that of a Th atom and six N_2 molecules.¹⁴ The calculated reaction energy for the decay of $\text{Fe}(\text{N}_5)_2$ into the most stable products of an Fe atom and five N_2 molecules was predicted to be 45 kcal/mol per N_2 unit.¹⁶ The present calculation on the dissociation of $\text{Ni}(\text{N}_4)_2$ into a Ni atom and 4N_2 is 52.5 kcal/mol per N_2 unit including ZPE correction (as shown in Table 3). It seems that $\text{Ni}(\text{N}_4)_2$ is energetically substantially higher than the predicted ScN_7 , ThN_6 , N_5ThN_7 , and $\text{Fe}(\text{N}_5)_2$. If $\text{Ni}(\text{N}_4)_2$ could be prepared, it would be an effective HEDM.

From the results presented in Tables 1 and 2, it is noted that the theoretically predicted geometries (minimum or saddle point) and relative energies are dependent upon the methods and basis sets employed, which have also been pointed out by other authors.^{9,37} It should be mentioned that electron correlation plays an important role in these Ni complexes. Moreover, larger basis sets produce more accurate descriptions of electrons that are very important for these complexes containing metal–ligand interaction. Considering that the MP2 method is usually liable in overestimating the electron correlation effect and both 6-311+G* and 6-311+G(3df,3pd) involve diffuse functions, our view at present is that the results obtained at the B3LYP/6-311+G* and B3LYP/6-311+G(3df,3pd) levels of theory are preferable to those obtained at the MP2/6-31G* and B3LYP/6-31G* levels of theory. However, for $\text{Ni}(\text{C}_4\text{H}_4)_2$ with D_{4d}

symmetry, the B3LYP/6-311+G* level of theory predicts it to be a minimum while the B3LYP/6-311+G(3df,3pd) predicts it to be a transition state. We then optimized the geometries of the staggered and eclipsed conformers of $\text{Ni}(\text{C}_4\text{H}_4)_2$ and performed frequency analyses at the B3LYP/6-311+G(3df,3pd) level of theory. The calculated result suggests that the eclipsed conformer is a local minimum while the staggered one is a transition state. That B3LYP and B3LYP methods give the identical result with the same 6-311+G(3df,3pd) basis set suggests the importance of the inclusion of the f-function in the present calculation.

In $\text{Ni}(\text{C}_4\text{H}_4)_2$ (the following discussions focus on the conformation of D_{4h} symmetry, until otherwise stated), all bond lengths of C–C bonds are equal, being close to those of $\text{C}_4\text{H}_4^{2-}$ (D_{4h}). NBO analysis shows that the WBIs for all C–C bonds in $\text{Ni}(\text{C}_2\text{H}_4)_2$ are 1.2, which suggests that there exists strong electronic delocalization in the vicinity of the two C_4 ring planes. The covalent radius value for carbon is 0.77 Å.³⁶ The bond length of Ni–C in $\text{Ni}(\text{C}_4\text{H}_4)_2$ is close to the sum of the covalent radii of nickel and carbon (1.98 Å). In $\text{Ni}(\text{C}_4\text{H}_4)_2$, it should be mentioned that all H atoms tip slightly out of the C_4 ring plane, bending away from the nickel atom by a small degree. At the B3LYP/6-31G* level of theory, Mulliken charge analysis shows that all positive charges lie on the nickel (about +0.23), all

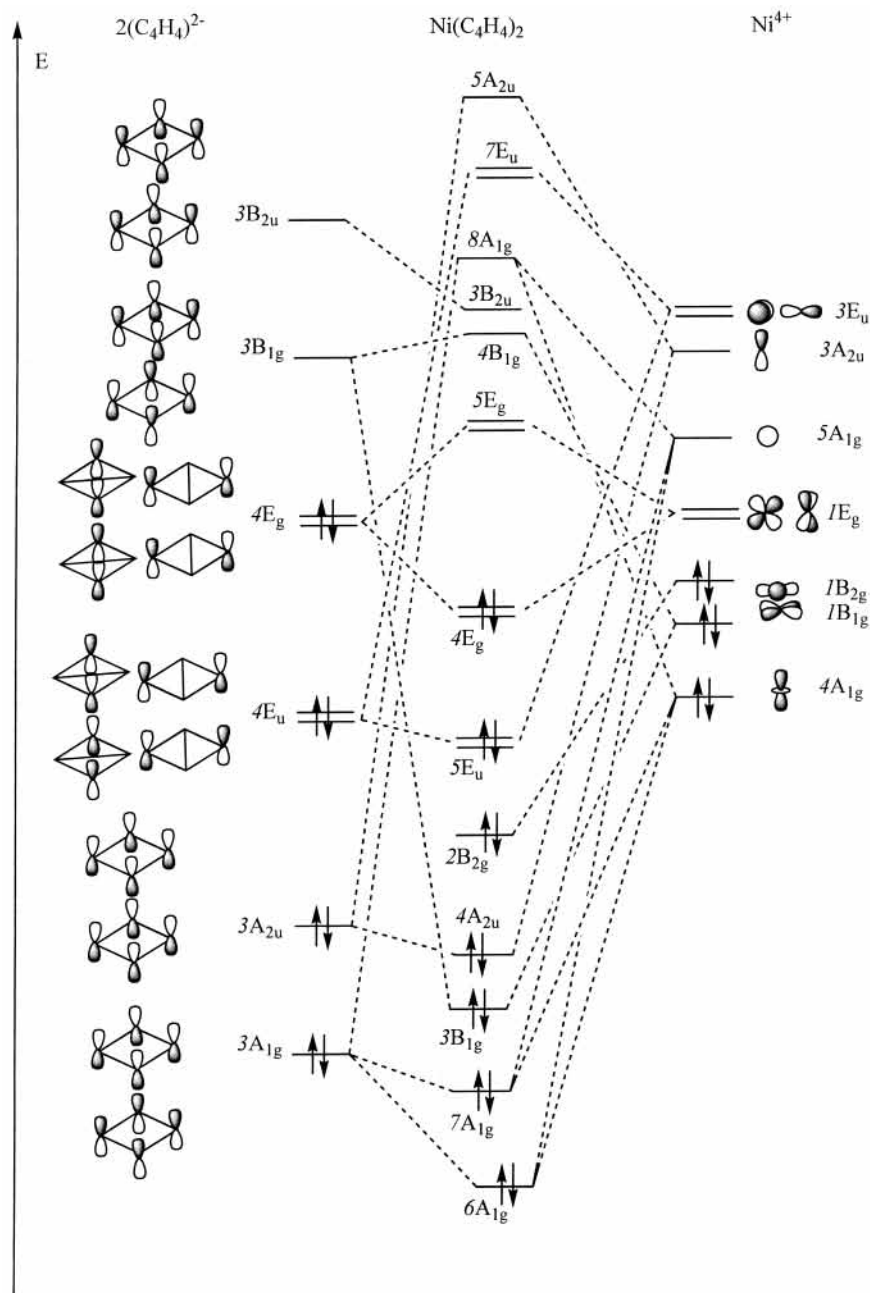


Figure 6. A qualitative frontier molecular orbital correlation diagram for $\text{Ni}(\text{C}_4\text{H}_4)_2$ (D_{4h}).

negative charges populate on the carbons (about -0.03), while no net charges lie on the hydrogens.

$\text{Ni}(\text{C}_2\text{O}_2)_2$, isoelectron with $\text{Ni}(\text{N}_4)_2$ and $\text{Ni}(\text{C}_4\text{H}_4)_2$, is an isomer of the known nickel carbonyl $\text{Ni}(\text{CO})_4$ (T_d). The bond length of C–O in the $\text{Ni}(\text{C}_2\text{O}_2)_2$ is close to that of $\text{C}_2\text{O}_2^{2-}$ (D_{2h}). The bond length of Ni–C is close to the sum of the covalent radii of the nickel and carbon atoms (1.98 Å). To assess the reliability of our computation, we also optimized the structure of the known $\text{Ni}(\text{CO})_4$. For $\text{Ni}(\text{CO})_4$ (T_d), our calculated Ni–C bond length is 1.774 (MP2/6-31G*), 1.811 (B3LYP/6-31G*), 1.846 (B3LYP/6-311+G*), and 1.852 Å (BHLYP/6-311+G-(3df,3pd)), while the C–O bond length is 1.162, 1.146, 1.138, and 1.119 Å at the above four levels of theory, respectively. The available experimental bond lengths of Ni–C and C–O in $\text{Ni}(\text{CO})_4$ are 1.838 and 1.141 Å, respectively.³⁸ Our calculated bond lengths at the B3LYP/6-311+G* level of theory are in good agreement with the experimental values. Note that the

ligand in $\text{Ni}(\text{C}_2\text{O}_2)_2$ is not a planar ring with a small dihedral angle.

In addition, we also investigated $\text{Ni}(\text{N}_2)_4$, an isomer of $\text{Ni}(\text{N}_4)_2$ with four end-on bonded N_2 ligands. The bond length of Ni–N is close to the sum of the covalent radii of nickel and nitrogen atoms (1.91 and 1.96 Å). The bond length of N–N is longer than the experimental triple-bond length of N_2 (1.098 Å).³⁹ NBO analysis shows that the WBIs for all N–N bonds in $\text{Ni}(\text{N}_2)_4$ are 2.7, while those for all Ni–N bonds are 0.4. According to Mulliken charge analysis, positive charges lie mainly on the nickel (about +0.41) and partly on the neighboring nitrogens (about +0.03 per N atom), while all negative charges populate on the terminal nitrogens (about -0.13 per N atom).

To estimate the strength of the interactions between the transition metal Ni and the ligands L (L = N_4^{2-} , $\text{C}_4\text{H}_4^{2-}$, $\text{C}_2\text{O}_2^{2-}$, N_2 , and CO), we performed the calculations on their

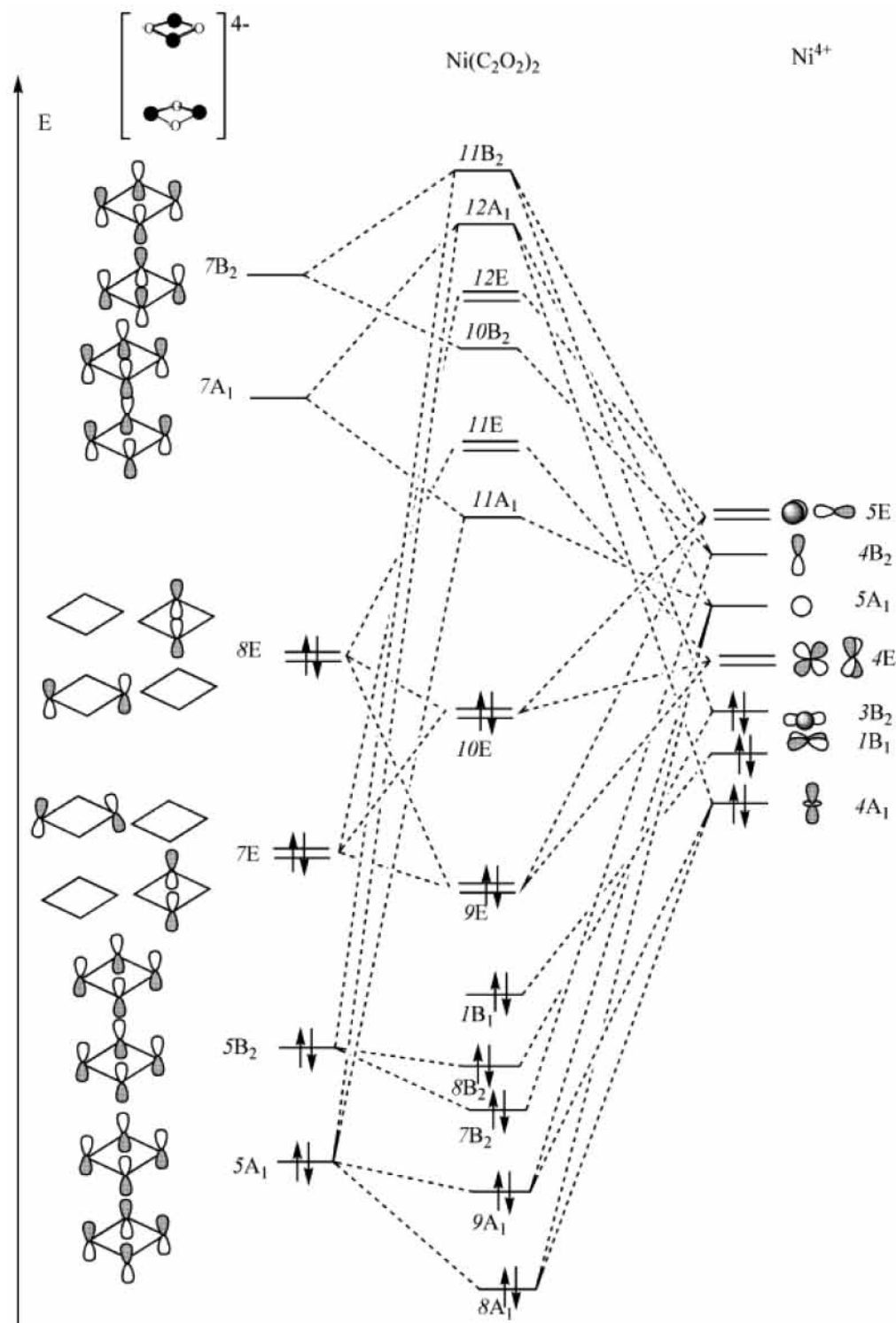


Figure 7. A qualitative frontier molecular orbital correlation diagram for $\text{Ni}(\text{C}_2\text{O}_2)_2$ (D_{2d}).

dissociation energies of the homolytic bond cleavage at the B3LYP/6-31G* level of theory. The results obtained are listed in Table 3. The average dissociation energies of the homolytic bond cleavage for $\text{Ni}(\text{N}_4)_2$, $\text{Ni}(\text{C}_4\text{H}_4)_2$, and $\text{Ni}(\text{C}_2\text{O}_2)_2$ are 71.2, 81.5, and 42.4 kcal/mol, respectively, after ZPE correction. It is obvious that the bond energy ordering is $\text{Ni}(\text{C}_4\text{H}_4)_2 > \text{Ni}(\text{N}_4)_2 > \text{Ni}(\text{C}_2\text{O}_2)_2$. This energy trend might be attributed to the following two facts: (1) The N_4^{2-} and $\text{C}_2\text{O}_2^{2-}$ rings both have large lone-pair repulsion, which comes from the N and O atoms, respectively. (2) The ligand $\text{C}_2\text{O}_2^{2-}$ in $\text{Ni}(\text{C}_2\text{O}_2)_2$ is not a planar ring, which may affect the strength of interaction between the ligand and metal. According to the average

dissociation energies of the homolytic bond cleavage for $\text{Ni}(\text{N}_2)_4$ and $\text{Ni}(\text{CO})_4$, we may come to a conclusion that the strength of the interaction between the metal and ligand in $\text{Ni}(\text{N}_2)_4$ (19.1 kcal/mol) is weaker than that in $\text{Ni}(\text{CO})_4$ (37.4 kcal/mol). The available experimental value for the homolytic bond cleavage energy for $\text{Ni}(\text{CO})_4$ is 140⁴⁰ or 144 kcal/mol,^{41,42} while our calculation result is 149.7 kcal/mol after ZPE correction, which agrees well with the experimental value. It can be seen from Table 3 that the $\text{Ni}(\text{C}_2\text{O}_2)_2$ is also high in energy, being 36 kcal/mol per CO unit higher with respect to its most stable dissociation products, a Ni atom and four CO molecules. As shown in Table 3, the dissociation of $\text{Ni}(\text{C}_4\text{H}_4)_2$ into a nickel

TABLE 1: Total Energies [au], Zero-Point Energies [kcal/mol],^a and Number of Imaginary Vibrational Frequencies^b of the Complexes Calculated at the MP2/6-31G*, B3LYP/6-31G*, B3LYP/6-311+G*, and BHLYP/6-311+G(3df,3pd) Levels of Theory and of the Transition States Calculated at the B3LYP/6-31G* Level of Theory

complexes	MP2/6-31G*	B3LYP/6-31G*	B3LYP/6-311+G*	BHLYP/6-311+G(3df,3pd)	B3LYP/6-311+G(3df,3pd) ^c
Ni(N ₄) ₂ (<i>D</i> _{4d})		-1945.83111 (21.3) (0)	-1946.07009 (20.9) (0)	-1945.67353 (22.8) (0)	
Ni(N ₄) ₂ (<i>D</i> _{4h})	-1943.53893 (87.8) (1)	-1945.82982 (21.1) (1)	-1946.06978 (20.7) (1)	-1945.67337 (22.6) (1)	
Ni(N ₂) ₄ (<i>T</i> _d)	-1944.08104 (19.3) (0)	-1946.28446 (18.9) (0)	-1946.57301 (18.5) (0)	-1946.18202 (19.1) (0)	
Ni(C ₄ H ₄) ₂ (<i>D</i> _{4h})	-1815.49681 (88.3) (1)	-1817.67406 (81.2) (1)	-1817.88106 (80.5) (0)	-1817.54734 (83.7) (0)	-1817.92389 (80.7) (0)
Ni(C ₄ H ₄) ₂ (<i>D</i> _{4d})	-1815.49772 (88.1) (0)	-1817.67596 (81.4) (0)	-1817.88066 (80.3) (0)	-1817.54650 (83.6) (1)	-1817.92341 (80.6) (1)
Ni(C ₂ O ₂) ₂ (<i>D</i> _{2d})	-1958.69998 (18.7) (0)	-1961.07145 (17.8) (0)	-1961.33945 (17.0) (0)	-1960.97509 (18.8) (0)	
Ni(CO) ₄ (<i>T</i> _d)	-1959.28060 (21.1) (0)	-1961.54774 (19.6) (0)	-1961.84005 (19.5) (0)	-1961.45982 (20.1) (0)	
TS1 (<i>C</i> ₁)		-1945.76883 (19.3) (1)			
TS2 (<i>C</i> ₂)		-1945.68993 (17.6) (1)			

^a In the first parentheses. ^b In the second parentheses. ^c Only the eclipsed and staggered conformers of Ni(C₄H₄)₂ were calculated at the B3LYP/6-311+G(3df,3pd) level of theory.

TABLE 2: Relative Energy [kcal/mol] with ZPE Corrections Calculated at the MP2/6-31G*, B3LYP/6-31G*, B3LYP/6-311+G*, and BHLYP/6-311+G(3df,3pd) Levels of Theory

complexes	MP2/ 6-31G*	B3LYP/ 6-31G*	B3LYP/ 6-311+G*	BHLYP/ 6-311+G(3df,3pd)	complexes	MP2/ 6-31G*	B3LYP/ 6-31G*	B3LYP/ 6-311+G*	BHLYP/ 6-311+G(3df,3pd)
Ni(N ₄) ₂ (<i>D</i> _{4d})		0.0	0.0	0.0	Ni(C ₄ H ₄) ₂ (<i>D</i> _{4d})	-0.8	-1.0	0.1	0.4
Ni(N ₄) ₂ (<i>D</i> _{4h})		0.6	-0.002	-0.1	Ni(C ₂ O ₂) ₂ (<i>D</i> _{2d})	0.0	0.0	0.0	0.0
Ni(N ₂) ₄ (<i>T</i> _d)		-286.9	-318.0	-322.8	Ni(CO) ₄ (<i>T</i> _d)	-361.0	-297.1	-311.6	-302.9
Ni(C ₄ H ₄) ₂ (<i>D</i> _{4h})	0.0	0.0	0.0	0.0					

TABLE 3: The Dissociation Energies [kcal/mol] of the Homolytic Bond Cleavage Calculated at the B3LYP/6-31G* Level of Theory

reactions	ΔH^a	ΔH with ZPE ^a	exptl value
Ni(N ₄) ₂ (<i>D</i> _{4d}) → Ni + 2N ₄ (<i>D</i> _{2h})	145.9 (72.9)	142.4 (71.2)	
Ni(C ₄ H ₄) ₂ (<i>D</i> _{4d}) → Ni + 2C ₄ H ₄ (<i>D</i> _{2h})	167.7 (83.8)	163.1 (81.5)	
Ni(C ₂ O ₂) ₂ (<i>D</i> _{2d}) → Ni + 2C ₂ O ₂ (<i>C</i> _{2v})	87.7 (43.8)	84.9 (42.4)	
Ni(N ₂) ₄ (<i>T</i> _d) → Ni + 4N ₂	81.2 (20.3)	76.3 (19.1)	
Ni(CO) ₄ (<i>T</i> _d) → Ni + 4CO	156.5 (39.1)	149.7 (37.4)	140, ^b 144 ^c
Ni(N ₄) ₂ (<i>D</i> _{4d}) → Ni + 4N ₂	-202.6 (-50.6)	-209.9 (-52.5)	
Ni(C ₂ O ₂) ₂ (<i>D</i> _{2d}) → Ni + 4CO	-139.1 (-34.8)	-144.1 (-36.0)	
Ni(C ₄ H ₄) ₂ (<i>D</i> _{4d}) → Ni + 4C ₂ H ₂ (<i>D</i> _{∞h})	200.8 (50.2)	186.2 (46.6)	

^a The average energies are listed in the parentheses. ^b Reference 40. ^c References 41 and 42.

atom and four C₂H₂ molecules is an endothermic reaction, which suggests that Ni(C₄H₄)₂ is not a high-energy species.

To understand the bonding between the metal and ligand in Ni(N₄)₂ (*D*_{4d}), as well as that in Ni(C₄H₄)₂ (*D*_{4h}) and Ni(C₂O₂)₂ (*D*_{2d}), qualitative frontier molecular orbital correlation diagrams calculated at the HF/STO-3G level of theory are shown in Figures 5–7, respectively. Our first expectation was that the bonding between the 2p π orbitals of the ligand and the d orbitals of the metal would be the main bonding scheme for these three complexes. To further explore the orbital interactions between the ligand and metal, we analyzed the contribution of the orbitals of the ligand and atomic orbitals (AOs) of the Ni⁴⁺ to the frontier molecular orbitals (MOs) of these three complexes. For Ni(N₄)₂, 39% of the 4E₂ MOs is from the 1E₂ AOs (d_{xy} and d_{x²-y²}) of the Ni⁴⁺ and only 0.4% is from the virtual 4E₂ orbitals of 2(N₄)²⁻ (besides, 54% is from the 3E₂ orbitals of 2(N₄)²⁻ composed of 2s and 2p hybrid orbitals that are not depicted in Figure 5), which suggests that the metal → ligand E₂ back-donation will be very weak. This might result from the high energy of the virtual 4E₂ orbitals of the ligand and the large positive charge of +4 of the metal. The 6E₁ MOs of Ni(N₄)₂ consist mainly of the orbitals of the ligand, including 22% from

the 4E₁ and 68% from the 3E₁ (3E₁ orbitals are formed from the 2s and 2p hybrid orbitals that are not depicted in Figure 5). The virtual 3E₁ AOs (p_x and p_y) of the metal only account for 3% of the 6E₁ MOs of Ni(N₄)₂, indicating that the ligand → metal E₁ donation will not be strong. This might be attributed to the fact that the virtual 3E₁ AOs of the Ni⁴⁺ are not as important acceptors as the empty d orbitals. The 4E₃ MOs of Ni(N₄)₂ consist mostly of the orbitals of the ligand, including 33% from the 4E₃ and 48% from the 3E₃ (3E₃ orbitals are formed from the 2s and 2p hybrid orbitals of 2(N₄)²⁻, which are not exhibited in Figure 5). The virtual 1E₃ AOs (d_{xz} and d_{yz}) of the Ni⁴⁺ account for 14% of the 4E₃ MOs of Ni(N₄)₂, suggesting that there exists strong ligand → metal π donation. This strong ligand → metal π donation contributes to stabilization of Ni(N₄)₂. For Ni(C₄H₄)₂, 73% of the 4E_g MOs is from the 4E_g orbitals of 2(C₄H₄)²⁻ and 20% is from the virtual 1E_g AOs (d_{xz} and d_{yz}) of the Ni⁴⁺. And 45% of the 5E_u MOs is from the 4E_u orbitals of the 2(C₄H₄)²⁻, and 32% is from the virtual 3E_u AOs (p_x and p_y) of the Ni⁴⁺. Obviously, there exist very strong ligand → metal π donations in Ni(C₄H₄)₂, which greatly contribute to stabilization of Ni(C₄H₄)₂. In addition, almost all of the 3B_{1g} MO of Ni(C₄H₄)₂ is from the 1B_{1g} AO

TABLE 4: Harmonic Vibrational Frequencies [cm⁻¹] and IR Intensities [km/mol] for Ni(N₄)₂ (D_{4d}), Ni(C₄H₄)₂ (D_{4d}), and Ni(C₂O₂)₂ (D_{2d}) at the B3LYP/6-31G* Level of Theory^a

Ni(N ₄) ₂ (D _{4d})			Ni(C ₄ H ₄) ₂ (D _{4d})			Ni(C ₂ O ₂) ₂ (D _{2d})		
mode	freq	IR	mode	freq	IR	mode	freq	IR
B ₁	51	0	B ₁	64	0	B ₁	92	0
E ₁	169	2	E ₁	146	4	E	113	2
A ₁	383	0	A ₁	373	0	E	257	0
E ₃	429	0	E ₃	435	0	A ₁	289	0
E ₁	473	9	E ₁	436	30	E	365	0
B ₂	619	38	B ₂	568	8	B ₂	452	1
E ₂	653	0	E ₂	633	0	A ₁	520	0
E ₁	951	2	E ₃	685	0	B ₂	567	1
E ₂	951	0	E ₁	732	0	A ₂	568	0
E ₃	960	0	E ₂	790	0	B ₁	652	0
E ₂	1156	0	B ₂	798	98	E	873	140
A ₁	1195	0	A ₁	801	0	E	940	152
B ₂	1199	3	E ₂	924	0	A ₁	972	0
			E ₃	955	0	B ₂	985	0
			E ₁	958	57	A ₁	1109	0
			E ₂	989	0	B ₂	1119	13
			A ₂	1186	0			
			B ₁	1188	0			
			E ₂	1204	0			
			B ₂	1263	45			
			A ₁	1267	0			
			E ₁	1359	2			
			E ₃	1367	0			
			E ₂	3254	0			
			E ₃	3272	0			
			E ₁	3272	15			
			B ₂	3289	0			
			A ₁	3289	0			

^a The intensities of degenerate modes have been doubled.

(d_{x²-y²) of the Ni⁴⁺, which indicates that there may be no B_{1g} back-donation from the Ni⁴⁺ to ligand. For Ni(C₂O₂)₂, 33% and 44% of the 10E MOs are from the 8E (composed of p_z orbitals of the C atoms) and 7E (composed of p_z orbitals of the O atoms) orbitals of the 2(C₂O₂)₂²⁻, and 4% and 15% are from the 5E (p_x and p_y) and 4E (d_{yz} and d_{yz}) AOs of the Ni⁴⁺, respectively. While 16% and 50% of the 9E MOs of Ni(C₂O₂)₂ are formed from the 8E and 7E orbitals of 2(C₂O₂)₂²⁻, 10% and 9% are from the 5E and 4E AOs of the Ni⁴⁺, respectively. Clearly, there exist very strong ligand → metal π donations, which greatly contribute to stabilization of Ni(C₂O₂)₂. In addition, almost all of the 8B₂ MO of Ni(C₂O₂)₂ is from 3B₂ (d_{xy}) AO of the metal, suggesting that there may be no B₂ back-donation from the Ni⁴⁺ to ligand. In conclusion, the MO component analyses show that there are strong ligand → metal π donations in Ni(N₄)₂, as well as in Ni(C₄H₄)₂ and Ni(C₂O₂)₂, which greatly contribute to their stabilizations.}

To facilitate the identification of the three NiL₂ (L = N₄²⁻, C₄H₄²⁻, and C₂O₂²⁻) complexes, harmonic vibrational frequencies and their associated IR intensities at the B3LYP/6-31G* level of theory are listed in Table 4.

4. Summary

In the present quantum chemical study, the geometries, energies, harmonic vibrational frequencies, and nature of bonding of three isoelectronic-liganded NiL₂ (L = N₄²⁻, C₄H₄²⁻, and C₂O₂²⁻) sandwich complexes were investigated by using the MP2 and DFT methods. Harmonic vibrational frequency analyses show that these three complexes are all local minima on their PES. The stable structure for Ni(N₄)₂ is a staggered conformer. The dissociation barriers at the B3LYP/6-31G* level of theory indicate that Ni(N₄)₂ is kinetically stable enough to resist dissociation. The calculated reaction energies for the

dissociation of Ni(N₄)₂, Ni(C₄H₄)₂, and Ni(C₂O₂)₂ into their respective stable products suggest that Ni(N₄)₂ and Ni(C₂O₂)₂ are high-energy species; however, Ni(C₄H₄)₂ is not. According to the qualitative frontier MO correlation diagrams and quantitative frontier MO component analyses, we may come to a conclusion that there exist strong ligand → metal π donations in Ni(N₄)₂, as well as in Ni(C₄H₄)₂ and Ni(C₂O₂)₂. These strong π donations greatly contribute to the stabilizations of the three complexes.

Supporting Information Available: Figure S-1 shows some molecular orbitals that correspond to the MO correlation diagram for Ni(N₄)₂ (D_{4d}). This material is available free of charge via the Internet at <http://pubs.acs.org>.

References and Notes

- Huber, H.; Ha, T. K.; Nguyen, M. T. *J. Mol. Struct. (THEOCHEM)* **1983**, *105*, 351.
- Gagliardi, L.; Orlandi, G. *J. Chem. Phys.* **2001**, *114*, 10733.
- Lauderdale, W. J.; Stanton, R. F.; Bartlett, R. J. *J. Phys. Chem.* **1992**, *96*, 1173.
- Glukhovtsev, M. N.; Jiao, H.; Schleyer, P. v. R. *Inorg. Chem.* **1996**, *35*, 7124.
- Christe, K. O.; Wilson, W. W.; Sheehy, J. A.; Boatz, J. A. *Angew. Chem., Int. Ed.* **1999**, *38*, 2004.
- Vij, A.; Wilson, W. W.; Vij, V.; Tham, F. S.; Sheehy, J. A.; Christe, K. O. *J. Am. Chem. Soc.* **2001**, *123*, 6308.
- Nguyen, M. T.; Ha, T. K. *Chem. Phys. Lett.* **2001**, *335*, 311.
- Gagliardi, L.; Evangelisti, S.; Barone, V.; Roos, B. O. *Chem. Phys. Lett.* **2000**, *320*, 518.
- Li, Q. S.; Zhao, J. F. *J. Phys. Chem. A* **2002**, *106*, 5928.
- Chung, G.; Schmidt, M. W.; Gordon, M. S. *J. Phys. Chem. A* **2000**, *104*, 5647.
- Strout, D. L. *J. Phys. Chem. A* **2002**, *106*, 816.
- Wilson, K. J.; Perera, S. A.; Bartlett, R. J.; Watts, J. D. *J. Phys. Chem. A* **2001**, *105*, 7693.
- Gagliardi, L.; Pyykkö, P. *J. Am. Chem. Soc.* **2001**, *123*, 9700.
- Gagliardi, L.; Pyykkö, P. *J. Phys. Chem. A* **2002**, *106*, 4690.
- Straka, M. *Chem. Phys. Lett.* **2002**, *358*, 531.
- Lein, M.; Frunzke, J.; Timoshkin, A.; Frenking, G. *Chem.—Eur. J.* **2001**, *7*, 4155.
- Zandwijk, G. v.; Janssen, R. A. J.; Buck, H. M. *J. Am. Chem. Soc.* **1990**, *112*, 4155.
- Kealy, T. J.; Pauson, P. L. *Nature* **1951**, *168*, 1039.
- Miller, S. A.; Tebboth, J. A.; Tremaine, J. F. *J. Chem. Soc.* **1952**, 632.
- Haslett, T. L.; Fedrigo, S.; Bosnick, K.; Moskovits, M.; Duarte, H. A.; Salahub, D. *J. Am. Chem. Soc.* **2000**, *122*, 6039.
- Duarte, H. A.; Salahub, D. R.; Haslett, T.; Moskovits, M. *Inorg. Chem.* **1999**, *38*, 3895.
- Becke, A. D. *J. Chem. Phys.* **1993**, *98*, 5648.
- Lee, C.; Yang, W.; Parr, R. G. *Phys. Rev. B* **1988**, *37*, 785.
- The BHandHLYP method implemented in the Gaussian programs has the formula 0.5 × Ex (LSDA) + 0.5 × Ex (HF) + 0.5 × Delta - Ex (B88) + Ec (LYP), which is actually somewhat different from the formulation proposed by Becke in his paper. Becke, A. D. *J. Chem. Phys.* **1993**, *99*, 1053.
- Møller, C.; Plesset, M. S. *Phys. Rev.* **1934**, *46*, 618.
- Binkley, J. S.; Pople, J. A. *Int. J. Quantum Chem.* **1975**, *9*, 229.
- Hehre, W. J.; Radom, L.; Schleyer, P. v. R.; Pople, J. A. *Ab initio Molecular Orbital Theory*; Wiley: New York, 1986.
- Carpenter, J. E.; Weinhold, F. *J. Mol. Struct. (THEOCHEM)* **1988**, *169*, 41.
- Reed, A. E.; Curtiss, L. A.; Weinhold, F. *Chem. Rev.* **1988**, *88*, 899.
- Foster, J. P.; Weinhold, F. *J. Am. Chem. Soc.* **1980**, *102*, 7211.
- Reed, A. E.; Weinstock, R. B.; Weinhold, F. *J. Chem. Phys.* **1985**, *83*, 735.
- Gonzalez, C.; Schlegel, H. B. *J. Phys. Chem.* **1990**, *94*, 5523.
- Frisch, M. J.; Trucks, G. W.; Schlegel, H. B.; Scuseria, G. E.; Robb, M. A.; Cheeseman, J. R.; Zakrzewski, V. G.; Montgomery, J. A., Jr.; Stratmann, R. E.; Burant, J. C.; Dapprich, S.; Millam, J. M.; Daniels, A. D.; Kudin, K. N.; Strain, M. C.; Farkas, O.; Tomasi, J.; Barone, V.; Cossi, M.; Cammi, R.; Mennucci, B.; Pomelli, C.; Adamo, C.; Clifford, S.; Ochterski, J.; Petersson, G. A.; Ayala, P. Y.; Cui, Q.; Morokuma, K.; Malick, D. K.; Rabuck, A. D.; Raghavachari, K.; Foresman, J. B.; Cioslowski, J.; Ortiz, J. V.; Stefanov, B. B.; Liu, G.; Liashenko, A.; Piskorz, P.; Komaromi, I.; Gomperts, R.; Martin, R. L.; Fox, D. J.; Keith, T.; Al-Laham, M. A.;

Peng, C. Y.; Nanayakkara, A.; Gonzalez, C.; Challacombe, M.; Gill, P. M. W.; Johnson, B. G.; Chen, W.; Wong, M. W.; Andres, J. L.; Head-Gordon, M.; Replogle, E. S.; Pople, J. A. *Gaussian 98*, revision A.9; Gaussian, Inc.: Pittsburgh, PA, 1998.

(34) Eluvathingal, D. J.; Boggavarapu, K. *Inorg. Chem.* **1998**, *37*, 2110.
(35) *Periodic Table of Elements*; Wiley-VCH: Weinheim, Germany, 1997.

(36) Huheey, J. E.; Keiter, E. A.; Keiter, R. L. *Inorganic Chemistry*; HarperCollins College Publishers: New York, 1993; p 292.

(37) Xie, Y.; Schaefer, H. F.; Fu, X.; Liu, R. *J. Chem. Phys.* **1999**, *111*, 2532.

(38) Pierloot, K.; Tsokos, E.; Vanquickenborne, L. G. *J. Phys. Chem.* **1996**, *100*, 16545.

(39) Lide, C. R. *CRC Handbook of Chemistry and Physics*, 73rd ed.; CRC Press: Boca Raton, FL, 1992.

(40) Fischer, A. K.; Cotton, F. A.; Wilkinson, G. *J. Am. Chem. Soc.* **1957**, *79*, 2044.

(41) Ross, W.; Hayne, F. H.; Hochman, R. F. *J. Chem. Eng. Data* **1964**, *9*, 339.

(42) Jones, L. H.; McDowell, R. S.; Goldblatt, M. *J. Chem. Phys.* **1968**, *48*, 2663.